Photothermally Controlled Structural Switching in Fluorinated Polyenes-Graphene Hybrids

Giovanni Bruno,* Giuseppe V. Bianco, Maria M. Giangregorio, Maria Losurdo and Pio Capezzuto

Supporting Information

Section 1 - Plasma fluorination of graphene

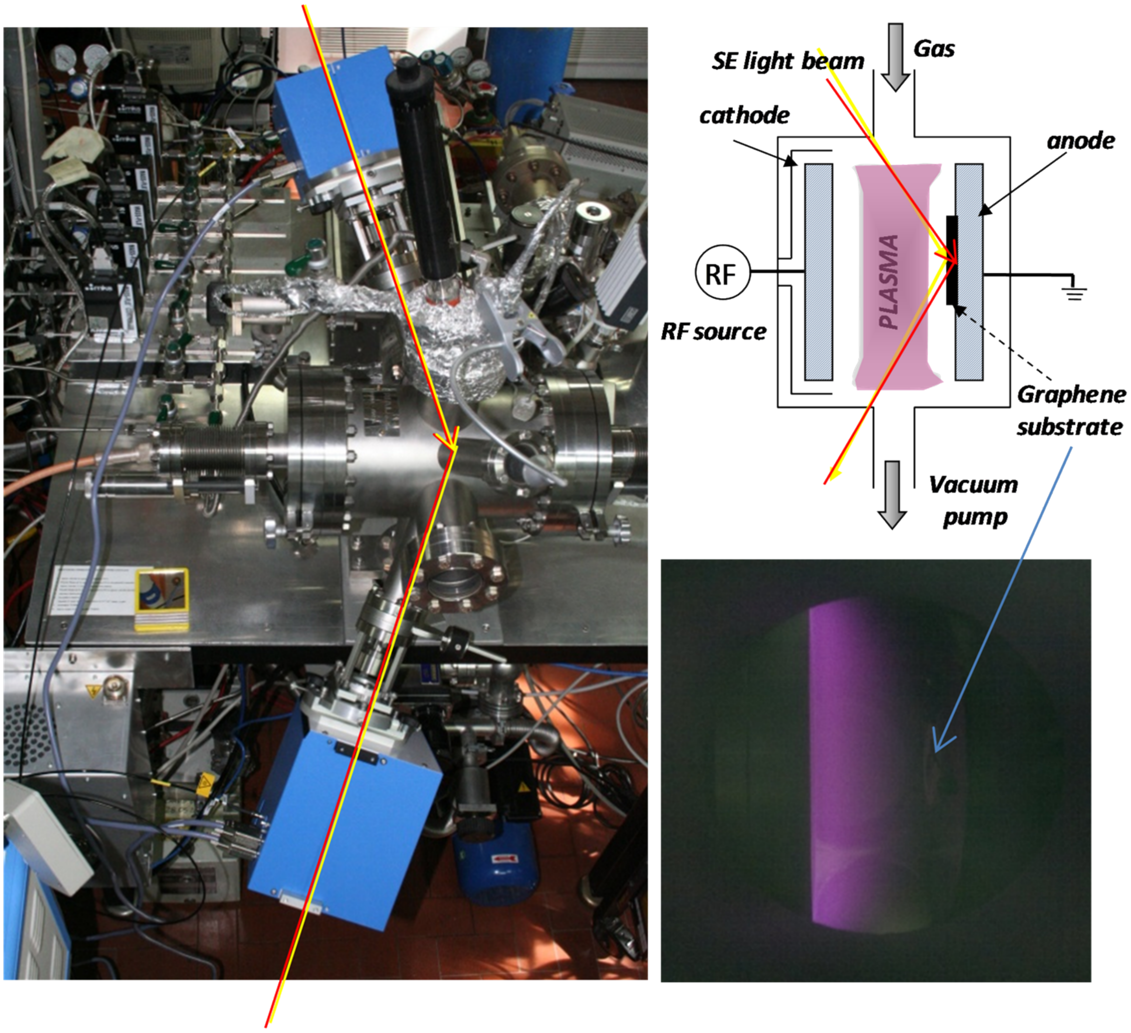

Figure S1.1-Plasma Reactor "Goldage" for graphene fluorination. The plasma chamber is a typical parallel plate configuration fed with a 13.54 MHz generator through a matching box. The plasma can be operated in continuous wave (CW) and in modulated wave (MW) conditions up to 10 KHz with variable duty cycles.

In the picture, the *in situ* phase modulated spectroscopic ellipsometer (the two cyan boxes), operating in the 1.5-5.5 eV spectral range, used for the *real time* monitoring of the graphene fluorination can be seen assembled on the chamber at an angle of incidence of 70°.The inset shows the typical plasma glow during fluorination .

Section 2 - Optical Response of Fluorinated CVD Graphene by spectroscopic ellipsometry

The optical response of graphene and fluorinated graphene on glass was revealed by spectroscopic ellipsometry.

Ellipsometry is based on measurements of the changes in light polarization upon reflection from a sample surface [1]. Linearly polarized light with known polarization impinges on the samples at an angle of incidence (70° in the present case), becoming elliptically polarized upon reflection depending on the optical properties of the surface. Indeed, the two components of the electromagnetic field-in the plane of incidence (p), and perpendicular (s) to the plane of incidence-experience different attenuation $\left|\frac{r_p}{r_s}\right|$ and phase shifts at the reflection (see **Fig. S2.1**). Those variations are described by $\tan\Psi$ that represents the absolute value $\left|\frac{r_p}{r_s}\right|$, while the phase change between the two polarization is described by $\cos\Delta$. They relate to the material refractive index and dielectric function through Fresnel's law, being ρ the complex reflection coefficient for the parallel, p, and perpendicular, s, polarizations, defined as:

$$\rho = \tan\Psi e^{j\Delta} = r_p/r_s \qquad (1)$$

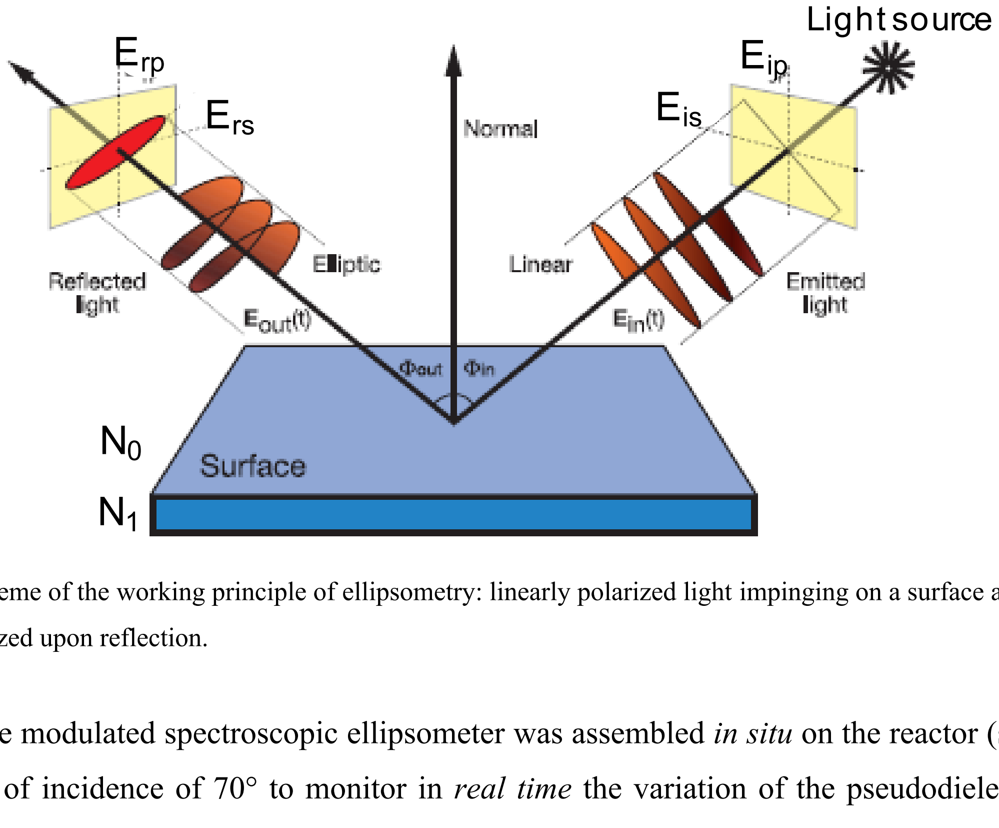

Figure S2.1. Scheme of the working principle of ellipsometry: linearly polarized light impinging on a surface and becoming elliptically polarized upon reflection.

A phase modulated spectroscopic ellipsometer was assembled *in situ* on the reactor (see Fig. S1.1) with an angle of incidence of 70° to monitor in *real time* the variation of the pseudodielectric function $\langle\varepsilon\rangle = \langle\varepsilon_r\rangle + i \langle\varepsilon_i\rangle$ of the graphene layer during fluorination. This *in situ* ellipsometer acquired $\langle\varepsilon\rangle$ spectra in the range 1.5 – 5.0 eV with a resolution of 0.05 eV and a time interval of 1 s. *In situ* data were complemented by *ex situ* additional ellipsometry measurements performed in a broader spectral range from 0.75 eV to 6.5 eV with a resolution of 0.01 eV and at variable angle of incidence.

The measured <ε> is related to the extinction coefficient, k, and to the refractive index, n, of the sample by the following equation

$$<\varepsilon>=<\varepsilon_r>+i<\varepsilon_i>=\sin^2\phi\left[1+\tan^2\phi\frac{(1-\rho)^2}{(1-\rho)^2}\right]=<(n+ik)^2> \qquad (2)$$

where ϕ is the angle of incidence and ρ is the complex reflection coefficient for the parallel, p, and perpendicular, s, polarizations, where $\tan\Psi$ represents the change of amplitude of the reflected polarized light beam with respect to the linearly polarized incident beam, while the phase change between the two polarizations is related to $\cos\Delta$. r_p and r_s are the Fresnel reflection coefficients (as defined in eq. (1)).

Spectroscopic ellipsometry has become a standard technique for the analysis of the optical properties of graphene, and more details can be found in refs. 1-4.

For monolayer graphene on glass, the experimental data were analyzed using a one-layer optical model consisting of a semi-infinite glass/graphene/air model using a point-by-point fitting, where the thickness of the graphene monolayer has been fixed to 3.4 Å expected from the interlayer spacing in graphite, and the extracted values were the refractive index, n, and extinction coefficient, k, which is related to the graphene absorption coefficient, $\alpha = 4\pi k/\lambda$. The glass substrate was back-roughed to eliminate back reflections and it was just measured before the transferring of graphene on it; this measured glass substrate entered the regression analysis to derive the optical constants of graphene.

Figure S2.2 shows the spectra of the refractive index and of the absorption coefficient, α, as a function of the fluorination time; for comparison, the spectra for exfoliated graphene from ref. [2] are also shown. The α spectrum of graphene is characterized by a prominent absorption peak at approximately 4.6 eV, which arises from the electronic transitions near the saddle M-point in the Brillouin zone of graphene [2]; correspondingly, a variation is seen in the Kramers-Kronig related spectrum of the refractive index, *n*. It can be seen that, under our fluorination conditions, there is no significant variation of the refractive index (consistently with the absence of graphene lattice damage supported by Raman spectroscopy for such fluorination times). Conversely, the modifications of the electronic properties of graphene, e.g. a reduction of the charge in the conducting π orbitals by fluorination, are seen in the decrease of the absorption coefficient with the increase in the fluorination time, consistently with previous reports [5].

Figure S2.3 also shows that the optical properties are sensitive to the cis-trans isomer transition of polyenes in the graphene lattice, consistently with modification of Raman spectra (see manuscript text). The change in the optical properties by the isomerization of polyenes domains in graphene is supported by the higher absorption coefficient of the trans-isomer than the cis-isomer of polyacetilenes well documented in literature [6].

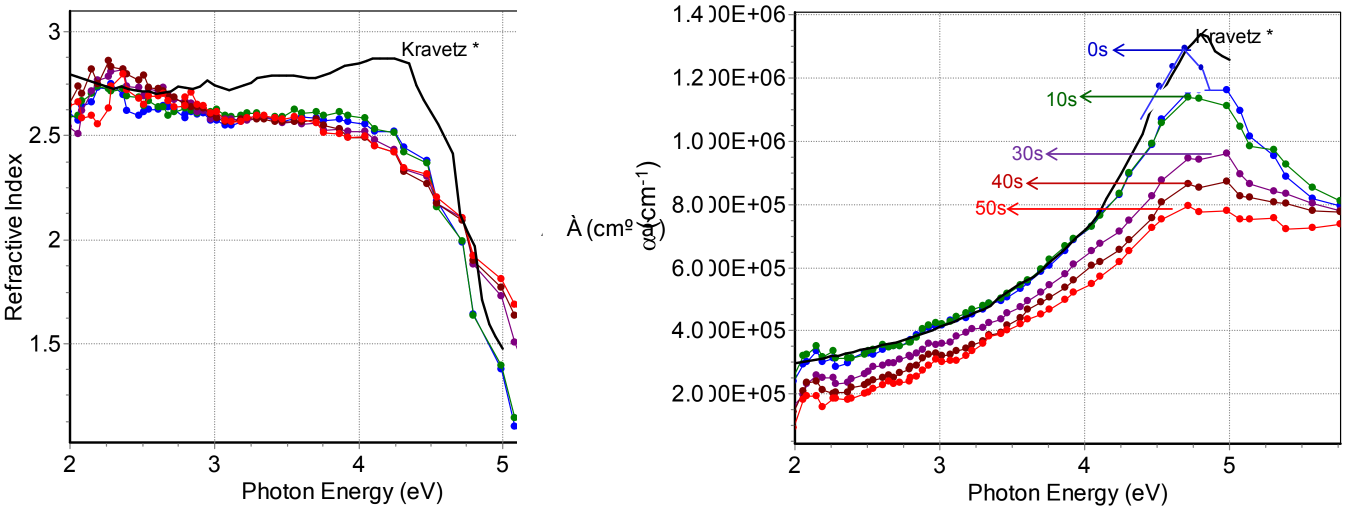

Figure S2.2. Spectra of the refractive index and absorption coefficient of graphene on glass as measured *in situ* and in *real time* as a function of fluorination time. For comparison, the optical constants for exfoliated graphene from Kravetz [2] are also shown.

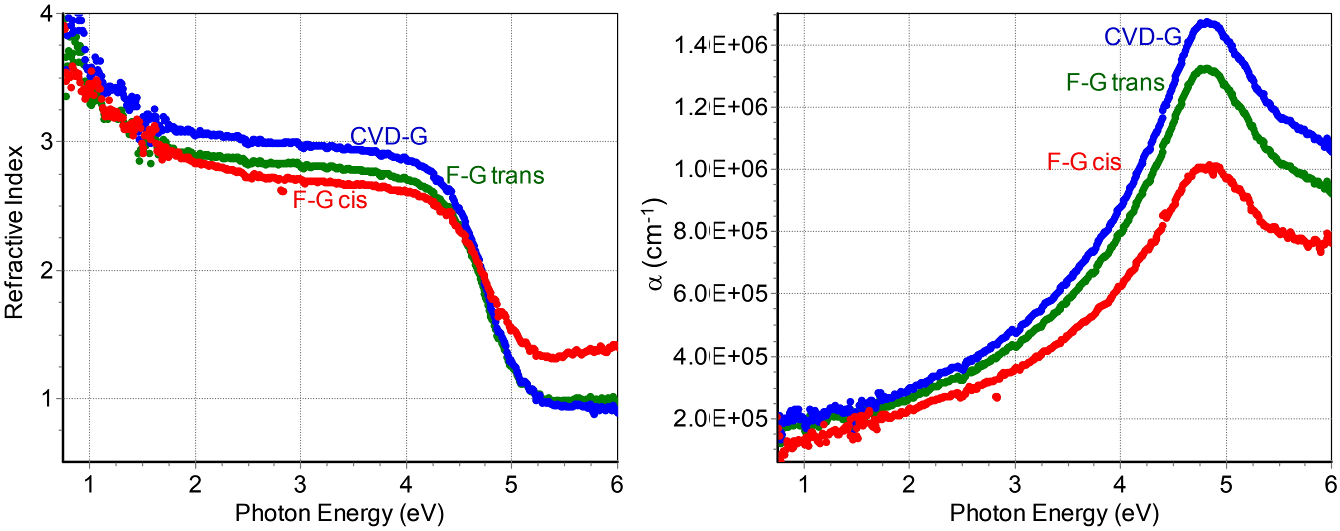

Figure S2.3. *Ex situ* spectra of the refractive index and absorption coefficient, α, of graphene on glass before (CVD-G, blue curves), after fluorination yielding the presence of cis----(F-G cis, red curves), and after annealing at 200°C resulting in the formation of trans---(F-G trans, green curves) polyenes.

Section 3 - Kelvin Probe Force Microscopy (KPFM).

The work function of fluorinated graphene (FG) samples was determined by an AutoProbe-CP, ThermoMicrocope operating in non-contact atomic force microscopy with an amplitude detection mode [7-9]. A gold-coated Si cantilever with a resonant frequency of 80 KHz was used. A modulation voltage with a frequency of 13 KHz and an amplitude variable in the range 1–5 V was applied between the tip and the sample. For the electrical connection to ground, a 50 nm gold layer was evaporated on FG, as shown in the scheme of Figure S3.1. The figure also shows the line profiles along the x-axis of the surface potential (SP) maps obtained scanning the tip from the FG to the evaporated Au contact, for two different samples. The SP of the evaporated Au contact is lower than the SP of fluorinated graphene. Since the SP is related to the difference between the work functions of the two different materials in contact, e.g. fluorinated graphene and gold [10, 11], from the SP profiles we found that the work function of FG is 640 ± 20 mV higher than that of the Au. Therefore, being 4.7 eV the work function of the evaporated Au contact, we estimated the work function of FG to be 5.34 ± 0.02 eV.

A similar value of 5.23 ±0.07 eV has been reported by Sherpa et al. for EG samples fluorinated by a SF_6 treatment in a reactive ion etcher (RIE) system [12].

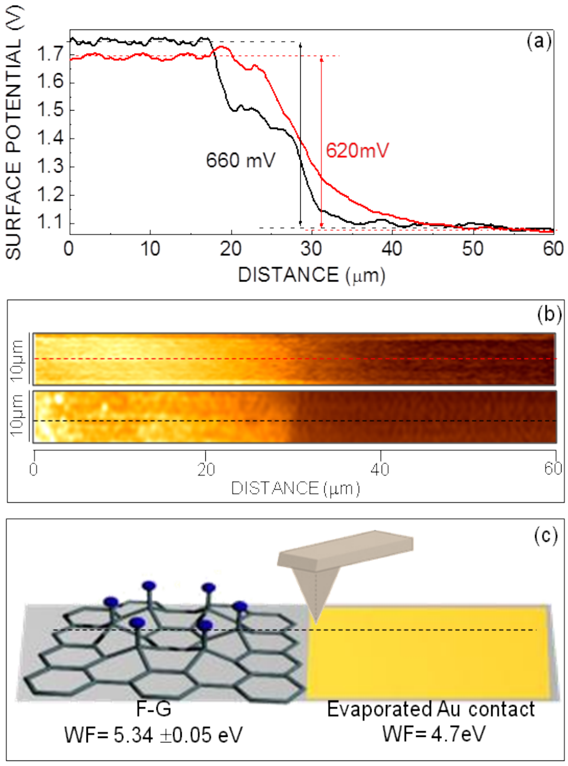

Figure S3.1. – KPFM of the graphene fluorinated for 300 sec (FG-300). (a) Line profiles, along the x-axis, of the surface potential (SP) between the fluorinated-graphene and the evaporated Au contact, measured for two different samples. (b) KPFM SP maps measured on two different samples to show reproducibility. The dotted lines correspond to the profiles shown in (a); (c) Scheme showing the sample structure: the graphene has been transferred onto glass and fluorinated and the Au contact has been deposited by evaporation on half of the sample. The calculated surface potential of fluorinated graphene is also shown at the bottom.

Section 4 - Electrical transport in fluorinated graphene

The transport properties of the fluorinated graphene were measured by d.c electrical measurements. They were carried out using the 4-point contacts van-der-Pauw geometry on a 5mmx5mm area of graphene on corning glass.

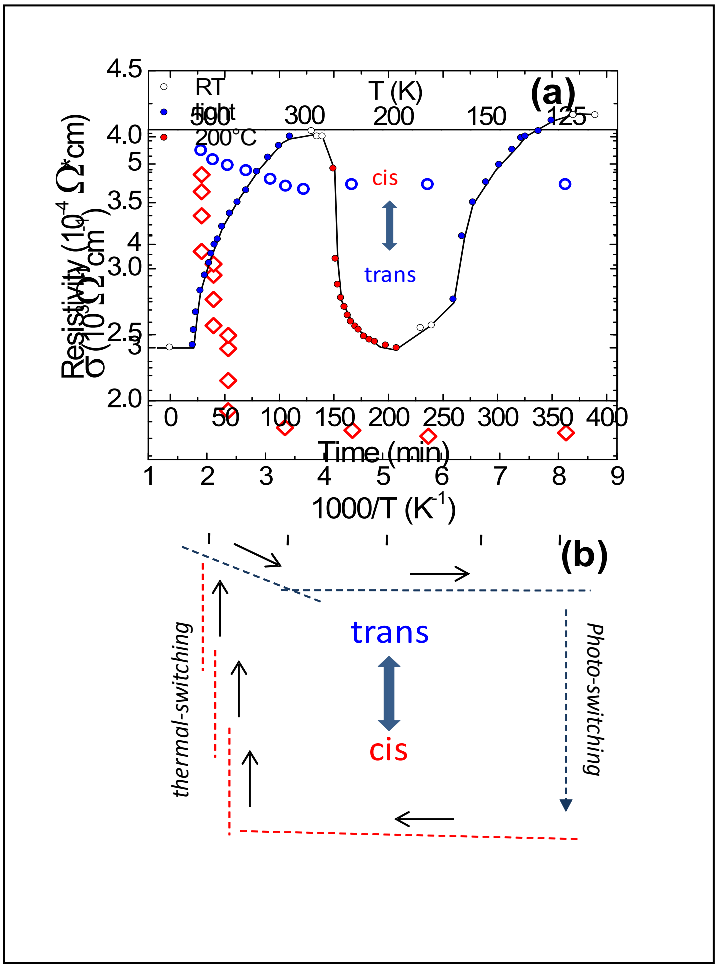

Figure S4.1– Electrical measurements of the graphene fluorinated for 25 sec (FG-25). (a) Variation of the resistivity, ρ, as a function of time also during cycles of white light irradiation (blue dots) and of annealing at 200°C (red-dots). (b) Arrhenius plot of the conductivity, of the trans-isomer (blue symbols) and of the cis-isomer (red symbols) obtained by light irradiation.

Section 5 – X-ray photoelectron spectroscopy analysis of fluorinated graphene

The chemical species analysis was run by x-ray photoelectron spectroscopy (XPS) using a XPS: Theta Probe (thermofisher) spectrometer equipped with a monochromatic Al *K*α x-ray source. The spot size was 300 μm. Spectral calibration was determined by setting the main C 1*s* component at 284.5 eV and the Au 4*f*7/2 line at 84.0 eV. Survey spectra were acquired with a pass energy 200eV, a step of BE 1eV, a dwell time of 50ms, and 15 periods. The main core photoelectron levels investigated were F1s, C1*s*, Si 2*p*, and O1*s*. Photoelectron core-levels spectra were acquired with pass energy of 20 eV. Figure S5.1 shows the survey spectrum of fluorinated graphene on glass, where only peaks due to fluorine and graphene and to the glass substrate are seen. From the survey, the atomic relative ratios were calculated resulting in F/C=0.3.

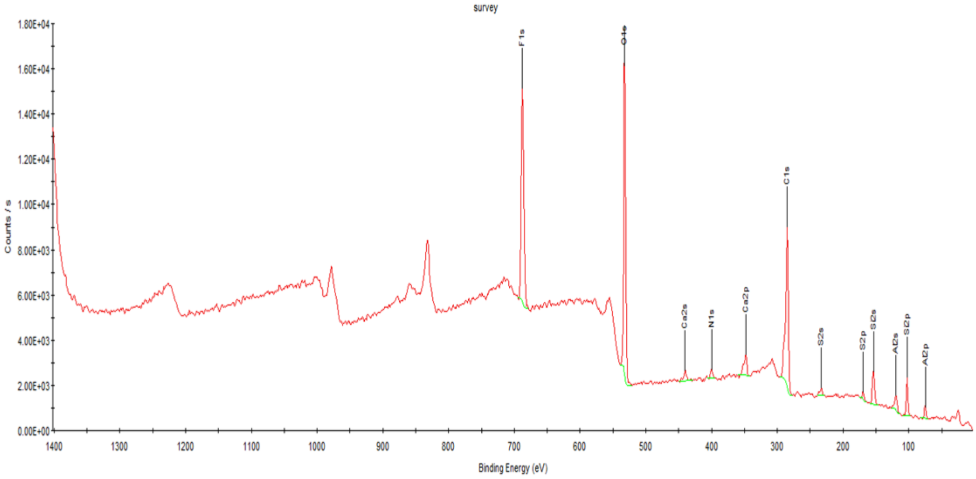

Figure S5.1– Survey XPS spectrum of fluorinated graphene on a glass susbtrate. F and C originate from te fluorinated graphene, while all the other peaks are from the glass susbtrate.

Figure S5.2 shows the C1s and F1s photoelectron core levels, with deconvoluted components in C1s at binding energy (BE) of 284.5 due to C-C and at 288.9 eV due to C-F bonds. The F1s is at BE of 687.6 eV, which also indicates C-F bonds.

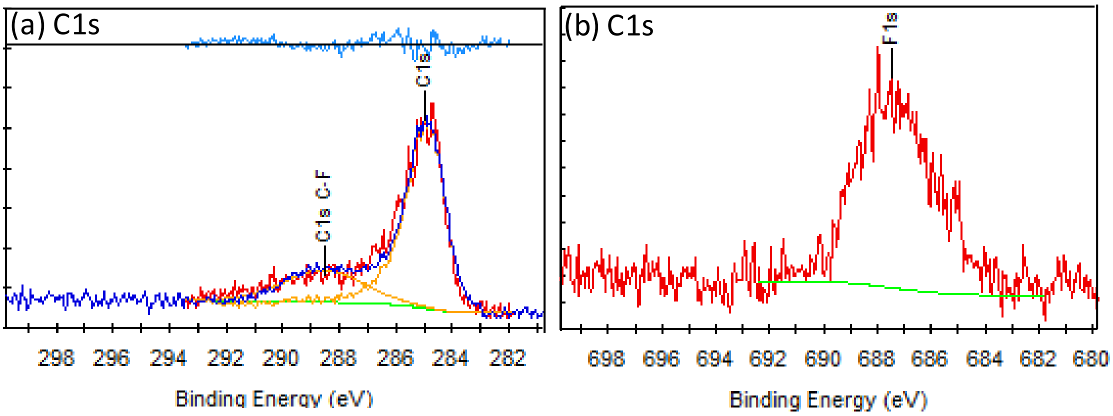

Figure S5.2– High-resolution (a) C1s and (b) F1s photoelectron core levels supporting the formation of C-F bonds.

Supporting References

_[1] M. Losurdo, M. Bergmair, G. Bruno, D. Cattelan, C. Cobet, A. de Martino, K. Fleischer, Z. Dohcevic-Mitrovic, N. Esser, M. Galliet, R. Gajic, D. Hemzal, K. Hingerl, J. Humlicek, R. Ossikovski, Z. V. Popovic, O. Saxl, Spectroscopic ellipsometry and polarimetry for materials and systems analysis at the nanometer scale: state-of-the-art, potential, and perspectives, *J. Nanopart. Res.* **2009**, *11*, 1521.

_[2] V. G. Kravets, A. N. Grigorenko, P. R. Nair, P. Blake, S. Anissimova, K. S. Novoselov and A. K. Geim, Spectroscopic ellipsometry of graphene and an exciton-shifted van Hove peak in absorption, *Phys. Rev. B,* **2010**, *81*, 155413.

_[3] A. Boosalis, T. Hofmann, V. Darakchieva, R. Yakimova, M. Schubert, Visible to vacuum ultraviolet dielectric functions of epitaxial graphene on 3C and 4H SiC polytypes determined by spectroscopic ellipsometry, *Appl. Phys. Lett.* **2012**, *101*, 011912.

_[4] M. Losurdo, M.M. Giangregorio, P. Capezzuto, G. Bruno, Ellipsometry as a Real-Time Optical Tool for Monitoring and Understanding Graphene Growth on Metals, *J. Phys. Chem. C* **2011**, *115*, 21804.

_[5] H. Eckhardt, On the optical properties of trans-polyacetylene, J. *Chem. Phys*. **1983**, *79*, 2085.

_[6] M. Tanaka, A.Watanabe, J. Tanaka, Absorption and Reflection Spectra of Pure and $ClSO_3H$ Dopd Polyacetylene Films, *Bull. Chem. Soc. Jpn.* **1980**, *53*, 3430.

_[7] Y. Shi, K.K. Kim, A. Reina, M. Hofmann, L.J. Li, J. Kong, Work function engineering of graphene electrode via chemical doping, *ACS Nano* **2010**, *4*, 2689.

_[8] N.J. Lee, J.W.Yoo, Y.J.Choi, C.J.Kang, D.Y. Jeon, D.C. Kim, S. Seo, H.J. Chung, The interlayer screening effect of graphene sheets investigated by Kelvin probe force microscopy, *Appl. Phys. Lett.* **2009**, *95*, 222107.

_[9] A.M. Zaniewski, M. Schriver, J.G. Lee, M.F. Crommie, A. Zettl, Electronic and optical properties of metal-nanoparticle filled graphene sandwiches, *Appl. Phys. Lett.* **2013**, *102*, 023108.

_[10] W.Melitz, J.Shen, A.C.Kummel, S.Lee, Kelvin probe force microscopy and its application, *Surf. Sc. Reports* **2011**, *66*, 1.

_[11] Y.Rosenwaks, R. Shikler, Th. Glatzel, S.Sadewasser, Kelvin probe force microscopy of semiconductor surface defects, *Phys. Rev. B* **2004**, *70*, 085320.

_[12] S.D.Sherpa, G.Levitin, D.W.Hess, Effect of the polarity of carbon-fluorine bonds on the work function of plasma-fluorinated epitaxial graphene, *Appl. Phys. Lett.* **2012,** *101*, 111602.